

Hysteresis in a Magnetic Bead and its Applications

Vanchna Singh and Varsha Banerjee

Department of Physics, Indian Institute of Technology,

Hauz Khas, New Delhi 110016, INDIA.

Abstract

We study hysteresis in a micron-sized bead: a non-magnetic matrix embedded with superparamagnetic nanoparticles. These hold tremendous promise in therapeutic applications as heat generating machines. The theoretical formulation uses a mean-field theory to account for dipolar interactions between the supermoments. The study enables manipulation of heat dissipation by a compatible selection of commercially available beads and the frequency f and amplitude h_o of the applied oscillating field in the laboratory. We also introduce the possibility of utilizing return point memory for gradual heating of a local region.

PACS numbers: 75.75.Jn, 76.60.Es, 75.60.-d

The use of small magnetic particles for diagnostic treatments is an emerging area of research. They provide several exciting opportunities for site-specific drug delivery, improving the quality of magnetic resonance imaging, manipulation of cell membranes, etc. [1–3]. The main reason behind this applicability is the ease with which they can be detected and directed by the application of an external magnetic field. They can be prepared in varying sizes, from nanometers to micrometers, comparable to the dimensions of biological entities such as genes, proteins, viruses and cells. When coated with relevant compounds, the particles can be made to bind to these entities thereby providing a controllable means of tagging them. The nanometer-sized particles are usually single-domain and superparamagnetic (SPM) in nature. Their relaxation behavior is characterized by Neel and Brownian relaxation times which are strongly size-dependent [4, 5]. The micron-sized particles, commonly called beads, are usually SPM particles packed in a non-magnetic matrix or a porous polymer with SPM particles precipitated in the pores [1, 6]. The micron-sized beads have several advantages over their nanometer-sized counterparts: they are easy to observe and manoeuvre and can be bound to cells due to their compatible dimensions.

When sufficiently large in number, the supermoments inside the bead start interacting via dipole-dipole coupling. They are no longer paramagnetic due to the appearance of a dipolar field. The presence of a permanent dipole moment opens up surprising avenues in biomedicine. An important non-equilibrium property exhibited by magnetic systems is that of hysteresis. Typically, when an oscillating magnetic field is applied, the response of the system is delayed leading to hysteresis. The magnitude of hysteresis is determined by the competition between experimental time scales (measured by the inverse frequency of the applied field) and the relaxation time scale of the magnetic moment. The area of the hysteresis loop is a measure of the heat dissipated in the system. The phenomenon of hysteresis can hence be advantageously used to heat magnetic beads positioned at a given site in the body, perhaps the site of malignancy, to selectively warm it! This effect, referred to as hyperthermia in the medical literature, makes it possible to destroy cells or introduce a modest rise in temperature to increase the efficiency of chemotherapy. While the possibility of using magnetic beads for hyperthermia holds tremendous promise, its successful application is a challenge as yet. The reason lies in the several complex questions which need to be answered in this context. For instance, what are the clinically acceptable values of the field amplitude and frequency of the applied oscillating field to attain maximal

heating? Or what should be the heat deposition rate to sustain tissue temperatures of 42° C or more? What is the adequate number of particles to be delivered at the specific site for achieving the required rise in temperature? It is therefore of great importance to understand heat generation and the role of tunable parameters for controlled heating of magnetic beads delivered on malignant cells.

In this letter we first motivate a mean field theory to incorporate the dipolar interactions between the magnetic nanoparticles embedded in the bead for the case of large uniaxial anisotropy *vis-a-vis* the thermal energy. The relaxation dynamics can then be described in terms of a two-state rate theory [7]. We study the role of volume fraction of SPM particles in the bead and the amplitude and frequency of the applied field on the hysteresis loop area. We quantify the dependence of loop area on the above parameters in the form of scaling laws. We also discuss the applicability of return point memory for progressive heating of a local region.

In the case of uniaxial anisotropy (in the z-direction say), the magnetic energy of a single-domain, SPM particle is given by [7]

$$E = VK \sin^2 \Phi, \quad (1)$$

where V is the magnetic volume of a particle, K is the effective magnetic anisotropy constant and Φ is the angle between the z-axis and direction of the “super” magnetic moment of the single-domain particle. Minimum energy occurs at $\Phi = 0$ and π and these angles define the two equilibrium orientations of the magnetic moment. If $VK \gg k_B T$, where k_B is the Boltzmann constant and T the absolute temperature, the magnetic moment is mostly locked in two minimum energy orientations resulting in the so-called Ising limit. In this limit, $\Phi(t)$ may be viewed as a dichotomic Markov process in which it jumps at random between the angles 0 and π . The jump rate governed by the Arrhenius-Kramer formula

$$\lambda_{0 \rightarrow \pi} = \lambda_{\pi \rightarrow 0} = \lambda_o \exp\left(-\frac{VK}{k_B T}\right), \quad (2)$$

where λ_o is the “attempt” frequency. The reciprocal of the jump rate is the Neel relaxation time τ_N .

In order to incorporate the effects of dipolar interactions, it is essential to add the contribution due to the “dipolar Hamiltonian” to the magnetic energy of the particle defined

by Eq. (1). In the limit of large anisotropy, this contribution is given by [8, 9]:

$$\mathcal{H}_d = \sum_{i,j} \gamma_i \gamma_j \hbar^2 \frac{(1 - 3\cos^2\theta_{ij})}{|r_{ij}|^3} m_{zi} m_{zj}, \quad (3)$$

where γ_i and γ_j are the gyromagnetic ratio of i^{th} and j^{th} particle respectively, $r_{ij}^{\vec{}}$ is the distance between the two particles, θ_{ij} is the angle between $r_{ij}^{\vec{}}$ and the anisotropy (z) axis and m_{zi} is the magnetic moment of the i^{th} nanoparticle along the anisotropy axis. Note that the angular dependence $(1 - 3\cos^2\theta_{ij})$ implies that the interaction can change sign thereby switching from ferromagnetic for angles close to the anisotropy axis to antiferromagnetic for intermediate angles ($55^\circ \leq \theta_{ij} \leq 125^\circ$). Since m is proportional to the volume of the particle, Eq. (3) can be rewritten as

$$\mathcal{H}_d = \gamma \hbar^2 \mu^2 V^2 \sum_j \gamma_j \frac{(1 - 3\cos^2\theta_{ij})}{|r_{ij}^{\vec{}}|^3} \cos\Phi_i \cos\Phi_j, \quad (4)$$

where μ is the magnetic moment per unit volume and Φ is as defined in Eq. (1).

A mean-field approach is invoked to treat the complicated interaction in Eq. (3) [9]. Each particle is visualized to be experiencing an effective local magnetic field H due to the surrounding (magnetic) medium. Further, the Ising limit allows for the replacement of $\cos\Phi$ by a two-state variable σ . These simplifications yield the mean-field dipolar Hamiltonian:

$$\mathcal{H}_d^{MF} = \mu V \sigma H, \quad (5)$$

with the field H evaluated self-consistently:

$$H = \mu \Lambda V \langle \sigma \rangle = \mu \Lambda V \tanh\left(\frac{\mu V H}{k_B T}\right). \quad (6)$$

The parameter Λ contains all the constants. It fluctuates in sign and has a magnitude dependent on the volume fraction of the SPM particles in the bead.

The presence of H alters Eq. (2). Neglecting terms of order H^2/K^2 due to the assumption of large anisotropy, yields the following generalized rate constants [10]:

$$\lambda_{0 \rightarrow \pi} = \lambda_0 \exp\left(-\frac{V(K + H\mu)}{k_B T}\right), \quad (7)$$

$$\lambda_{\pi \rightarrow 0} = \lambda_0 \exp\left(-\frac{V(K - H\mu)}{k_B T}\right). \quad (8)$$

The relative populations of magnetic moments aligned along and against the anisotropy axis (corresponding to $\Phi = 0$ and π) are now described by a master equation for a two-state

system [9]:

$$\frac{d}{dt}n_0(t) = -\lambda_{0\rightarrow\pi}n_0(t) + \lambda_{\pi\rightarrow 0}n_\pi(t), \quad (9)$$

where n_0 and n_π denote the fraction of particles with orientation 0 and π respectively. Solving Eq. (9), we can obtain the time-dependent magnetization

$$m(t) = V\mu[n_0(t) - n_\pi(t)]. \quad (10)$$

We now subject the bead to a time-dependent oscillating field $h(t) = h_o \cos 2\pi ft$. It is necessary to replace the dipolar mean-field H in the exponent of Eqs. (7) and (8) by a time-dependent field $\tilde{H}(t) = H + h(t)$. The hysteresis loop can then be obtained by evaluation of $m(t)$ using Eq. (10) at each value of the applied field $h(t)$. We allow $m(t)$ to evolve for a few cycles of the magnetic field to provide sufficient time for the transients to settle down. As the dipolar mean field H is weak, the magnetization reversal is primarily driven by the applied field $h(t)$. However we shall see that though weak in strength, it significantly affects the relaxation behavior of the magnetic bead.

It is appropriate to keep a note of the parameter values that are relevant in the context of local heating of cells using magnetic nanoparticles. The temperatures required in hyperthermia and chemotherapy treatments are usually in the range of $42^\circ C$ to $45^\circ C$ [1]. The frequency f of the applied oscillating magnetic field is in the 50 to 1500 KHz range and the field amplitude usually varies between 1 to 200 Oe [1]. Several groups have reported that exposure to fields with a product $h_o \cdot f$ not exceeding $4.85 \times 10^8 A m^{-1} s^{-1}$ is clinically safe [1]. We have ensured that our evaluations include the aforementioned ranges of frequency and field amplitude. Further, the problem of tissue cooling due to presence of blood flow is difficult to address due to its mathematical complexity. However an often-used thumb rule is that a heat deposition rate P of $100 mW cm^{-3}$ is sufficient in most situations [1].

Commercially available beads contain nanoparticles of iron, nickel or cobalt compounds with tailored volume fractions. Our numerical evaluations of the loop and its area have been made for beads comprising of magnetite (Fe_3O_4) nanoparticles having a diameter of 8 nm and an anisotropy constant of $4.68 \times 10^5 ergs/cm^3$ [11]. A 1% volume fraction in this case corresponds to the presence of approximately 10^4 magnetite nanoparticles in the micron-sized bead. For body temperature $T = 37^\circ C$, the Ising limit $VK \gg k_B T$ that we assume holds for diameters in the range 6 to 12 nm . We find that our qualitative observations

remain unchanged, even in the case of MNP of alternative compounds, as long as we work in this limit.

In Figure 1, we plot the response of the bead to the applied field $h(t)$ for several values of the volume fraction V_f . (i) At low volume fractions ($V_f \sim 1\%$), the supermoments continue to remain non-interacting and the reversal is governed by the Neel relaxation time. The magnetization curve is thus the Langevin function. (ii) As the volume fraction is increased, the supermoments begin to interact via dipole-dipole coupling. Our numerics indicate that the resulting mean field H is small for these volume fractions. As a consequence the rates $\lambda_{0 \rightarrow \pi}$ and $\lambda_{\pi \rightarrow 0}$ governed by Eqs. (7) and (8) respectively have comparable magnitudes and both contribute to the relaxation dynamics, especially near $h(t) \approx 0$. The approach to an all-up or an all-down configuration of the supermoments is thereby impeded, resulting in smooth and continuous hysteresis loops. (iii) For high volume fractions ($V_f \gtrsim 30\%$), the mean field H is large enough to make one of the relaxation rates dominate over the other for any value of $h(t)$. The system then exhibits a sharp reversal from an all-up to an all-down configuration and vice-versa under the action of the oscillating field $h(t)$.

Figure 2a shows the effect of the field frequency f on the hysteresis loop. Leaf-shaped loops are obtained when $f \sim \lambda$. These go over to elliptic loops with their major axis parallel to the h axis on increasing f . For $f \gg \lambda$, the supermoments are unable to respond to the field variation and no hysteresis loops are observed. Figure 2b shows the effect of the amplitude of the oscillating field h_o on the loops. Their shape ceases to depend on h_o when it is sufficiently large to produce saturated loops.

In Figure 3, we quantify the effects of V_f , f and h_o on the loop area in the form of a scaling law. Our numerical evaluations suggest a power law variation $A(V_f, f, h_o) \sim V_f^\alpha f^\beta h_o^\delta$ where the exponents α , β and δ are distinct for cases (ii) and (iii) discussed in the context of Figure 1. The values of these exponents are 1.3 ± 0.02 , 0.95 ± 0.02 and 1.5 ± 0.02 for case (ii) and 2.0 ± 0.02 , 0.9 ± 0.02 and 1.1 ± 0.02 for case (iii). The heat deposition rate P can be obtained from the loop area A via the relation $P = f \times A/V$ where V is the volume of the bead. This relationship enables us to identify the clinically useful range of the loop area which is indicated in the figure. The scaling law can therefore be utilized to select (several) triplets (V_f, f, h_o) to generate a desired heat deposition rate. Some of them, for the encircled values of A which yield $P \sim 100 \text{ mWcm}^{-3}$, have been provided in Table I.

Finally, we study the phenomenon of return point memory in the bead. If the field $h(t)$ is

made to cycle with a reduced amplitude to generate a sub-loop, the system returns precisely to the same state from which it left the outer loop. This same memory effect extends to sub-cycles within cycles. The system thus remembers a hierarchy of states in its past external fields. Figure 4 illustrates the return point memory effect in the magnetic bead. The inset evaluates the heat dissipated as a function of h_o , the maximal field amplitude used to generate the minor loops. We find that return point memory is always observed in standard leaf-shaped loops with saturation. This phenomenon, though unexplored in the context of hyperthermia, seems a promising technique for gradual heating of a local area.

In conclusion, the present letter elucidates hysteresis in a micron-sized bead described as a non-magnetic matrix embedded with superparamagnetic nanoparticles. The study enables manipulation of heat dissipation by a compatible selection of commercially available beads characterized by the volume fraction V_f of the superparamagnetic nanoparticles and the frequency f and amplitude h_o of the applied oscillating field in the laboratory. We hope that the simple mean field framework proves useful in efficient design of experiments in the context of therapeutic applications such as hyperthermia and chemotherapy. We also hope that this study provokes experiments on the utility of return point memory in these applications.

-
- [1] Q. A. Pankhurst, J. Connolly, S. K. Jones and J. Dobson, *J. Phys. D: Appl. Phys.* **36**, R167 (2003).
 - [2] S. Purushotham and R. V. Ramanujan, *J. Appl. Phys.* **107**, 114701 (2010).
 - [3] C. C. Berry and A. S. G. Curtis, *J. Phys. D: Appl. Phys.* **36**, R198 (2003); C. C. Berry, *J. Phys. D: Appl. Phys.* **42**, 224003 (2009).
 - [4] R. E. Rosensweig, *Ferrohydrodynamics* (Dover, New York, 1997).
 - [5] V. Singh, V. Banerjee and M. Sharma, *J. Phys. D: Appl. Phys.* **42**, 245006 (2009).
 - [6] M. L. Hans and A. M. Lowman, *Curr. Opin. Solid State Mater. Sci.* **6**, 319 (2002).
 - [7] S. Dattagupta, *Relaxation Phenomena in Condensed Matter Physics* (Academic Press, 1987).
 - [8] A. Abragam, *The theory of Nuclear Magnetism* (Oxford University Press, London, 1961).
 - [9] S. Chakraverty, M. Bandyopadhyay, S. Chatterjee, S. Dattagupta, A. Frydman, S. Sengupta and P. A. Sreeram, *Phys. Rev. B* **71**, 054401 (2005).

[10] A. Aharoni, Phys. Rev. **177**, 793 (1969).

[11] G. F. Goya, T. S. Berquo and F. C. Fonseca, J. Appl. Phys. **94**, 3520 (2003).

Table I

V_f (%)	h_o (Oe)	f (KHz)
10	200	1500 – 1800
15	150	1500 – 1800
15	200	800 – 1500
20	100	900 – 1500
20	150	600 – 1200
20	200	400 – 850
25	100	300 – 800
25	200	200 – 350

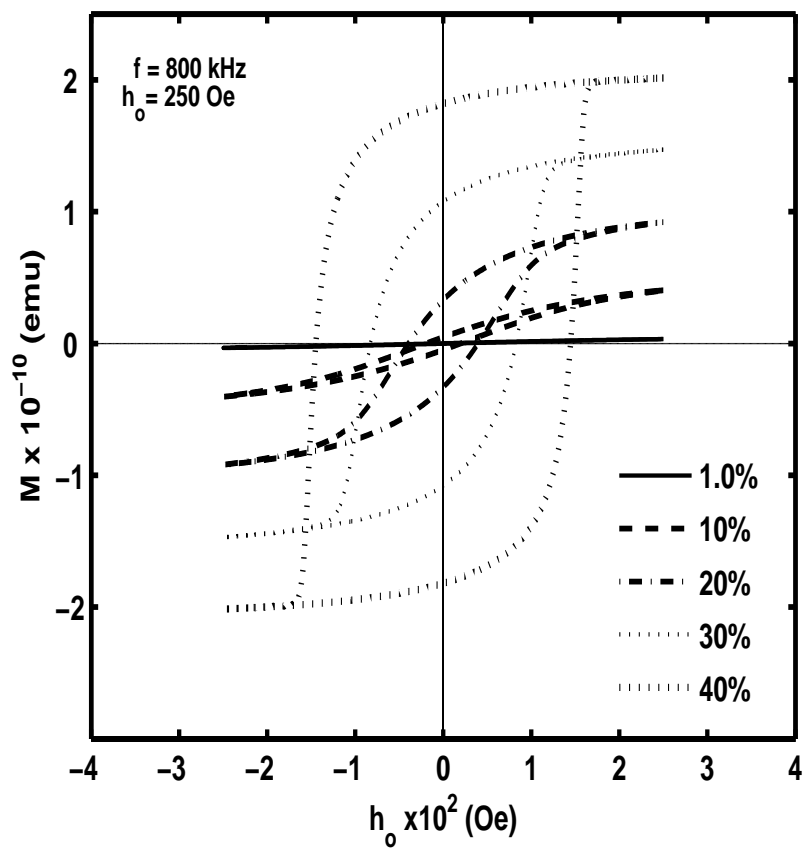


Figure 1

Figure 1: Typical hysteresis loops for several values of the volume fraction V_f specified in the figure.

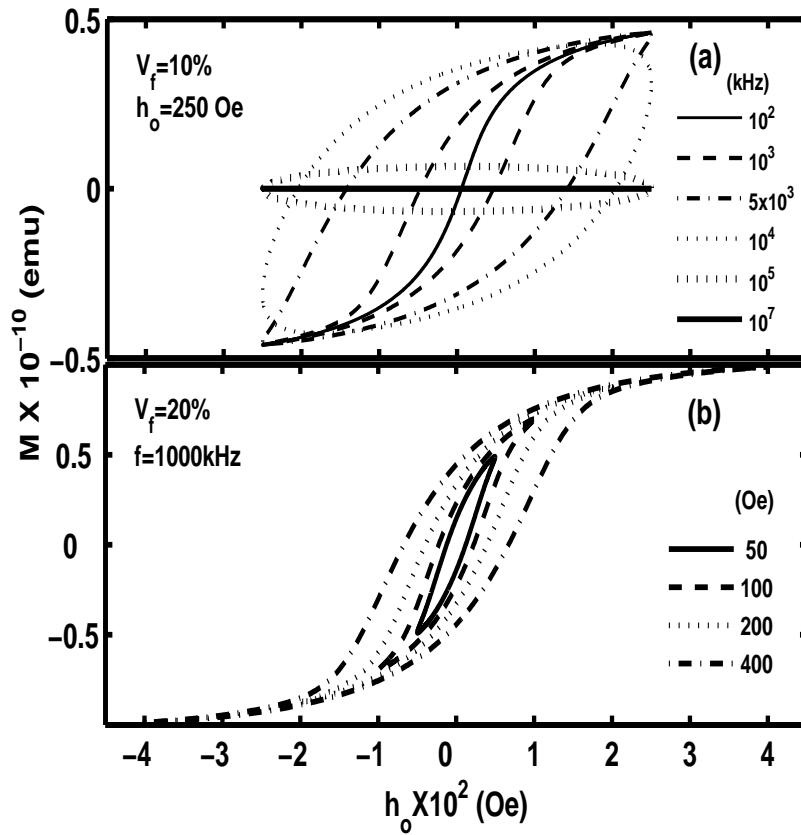


Figure 2

Figure 2: Variation in the hysteresis loop as a function of (a) the applied frequency f and (b) the amplitude h_o of the applied oscillating field.

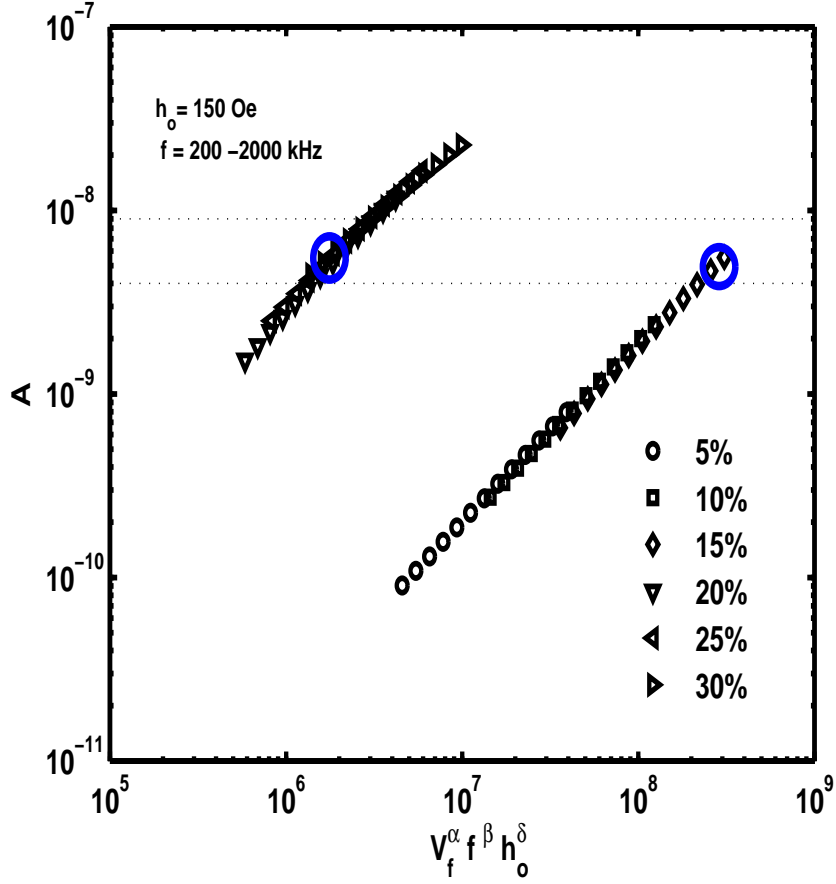


Figure 3

Figure 3: A scaling plot which demonstrates that the area of the hysteresis loop scales as $A(V_f, f, h_o) \propto V_f^\alpha f^\beta h_o^\delta$. The scaling exponents are specified in the text. The region within the dotted lines yields heat deposition suitable for hyperthermia. Several triplets (V_f, f, h_o) corresponding to the encircled value of A are specified in Table I.

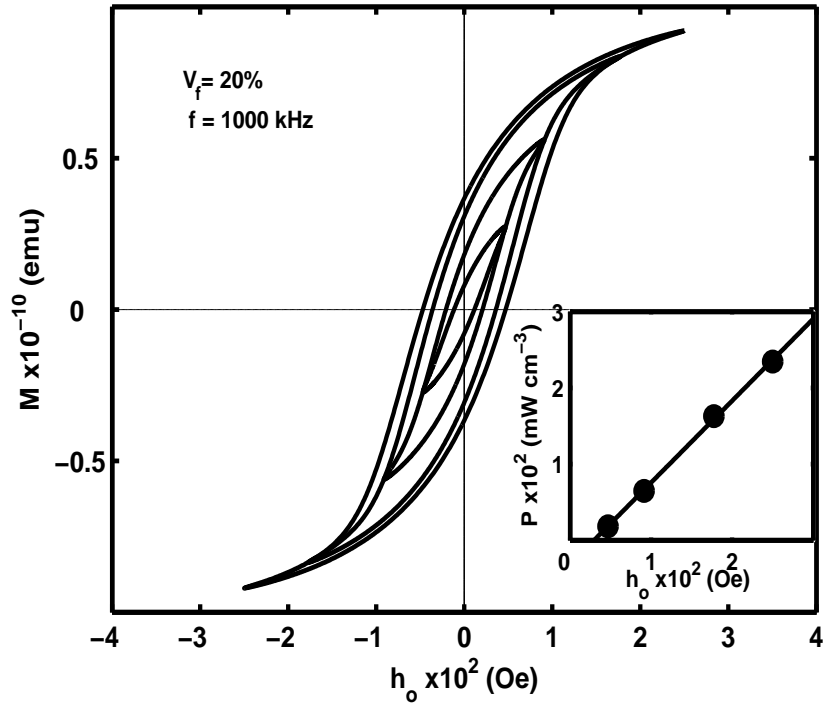


Figure 4

Figure 4: Hysteresis loop showing return point memory for several minor loops. The inset indicates the heat dissipated as a function of h_o , the maximum amplitude of the applied oscillating field for the minor loop.